HYDROGEN AND FUEL CELL STATIONARY APPLICATIONS: KEY FINDINGS OF MODELLING AND EXPERIMENTAL WORK IN THE HYPER PROJECT

S. Brennan[1], A. Bengaouer[2], M. Carcassi[3], G. Cerchiara[3], G. Evans[4], A. Friedrich[5], O. Gentilhomme[6], W. Houf[4], A. Kotchurko[7], N. Kotchourko[5], S. Kudriakov[2], D. Makarov[1], V. Molkov[1], E. Papanikolaou[8], C. Pitre[2], M. Royle[9], R. Schefer[4], G. Stern[5], A. Venetsanos[8], A. Veser[5], D. Willoughby[9], J. Yanez[7]

[1] HySAFER centre, University of Ulster, *sl.brennan@ulster.ac.uk*
[2] Heat Transfer and Fluid Mechanics Laboratory, CEA, France,
[3] University of Pisa, Italy, [4]Sandia National Laboratories, Livermore, CA USA,
[5] Pro-Science GmbH, Germany.
[6] Explosion-Dispersion Unit, INERIS, Verneuil-en-Halatte, France,
[7] IKET, Forschungszentrum Karlsruhe, Germany,
[8] Environmental Research Laboratory, National Centre for Scientific Research Demokritos, Greece,
[9] Health and Safety Laboratory, Harpur Hill, UK

ABSTRACT

This paper summarises the modelling and experimental programme in the EC FP6 project HYPER. A number of key results are presented and the relevance of these findings to installation permitting guidelines (IPG) for small stationary hydrogen and fuel cell systems is discussed. A key aim of the activities was to generate new scientific data and knowledge in the field of hydrogen safety, and, where possible, use this data as a basis to support the recommendations in the IPG. The structure of the paper mirrors that of the work programme within HYPER in that the work is described in terms of a number of relevant scenarios as follows: 1. high pressure releases, 2. small foreseeable releases, 3. catastrophic releases, and 4. the effects of walls and barriers. Within each scenario the key objectives, activities and results are discussed.

The work on high pressure releases sought to provide information for informing safety distances for high-pressure components and associated fuel storage, activities on both ignited and unignited jets are reported. A study on small foreseeable releases, which could potentially be controlled through forced or natural ventilation, is described. The aim of the study was to determine the ventilation requirements in enclosures containing fuel cells, such that in the event of a foreseeable leak, the concentration of hydrogen in air for zone 2 ATEX is not exceeded. The hazard potential of a possibly catastrophic hydrogen leakage inside a fuel cell cabinet was investigated using a generic fuel cell enclosure model. The rupture of the hydrogen feed line inside the enclosure was considered and both dispersion and combustion of the resulting hydrogen air mixture were examined for a range of leak rates, and blockage ratios. Key findings of this study are presented. Finally the scenario on walls and barriers is discussed; a mitigation strategy to potentially reduce the exposure to jet flames is to incorporate barriers around hydrogen storage equipment. Conclusions of experimental and modelling work which aim to provide guidance on configuration and placement of these walls to minimise overall hazards is presented.

1. INTRODUCTION

The HYPER project was aimed at developing for small stationary hydrogen (H_2) and fuel cell (FC) systems a fast track approval of safety and procedural issues, by providing a comprehensive agreed installation permitting process for developers, design engineers, manufacturers, installers and authorities having jurisdiction across the EU. The main output of the project was the Installation Permitting Guidance (IPG). The reader is referred to the IPG and supporting documents from the HYPER work packages for more detailed information [1-6]. The IPG includes an assessment of current knowledge on installation requirements, detailed case studies of representative installations and a synthesis of modelling and experimental risk evaluation studies. The HYPER project (Nov 2006- Dec 2008) was funded by the EC in the frame of FP6 as a specific targeted research project, and involved 15 partners from the European Community as well as Russia and USA. A complementary modelling and experimental programme was carried out. Following a gap analysis [6], a number of topics, relevant to small stationary H_2 and FC installations were addressed, including: 1. high and low

pressure releases, 2. foreseeable and catastrophic releases, 3. explosive atmospheres both inside and outside equipment casing, 4. explosive atmospheres inside a room or building, 5. quiescent or turbulent explosive atmospheres, 6. early and late ignition, 7. explosion or jet fire, and 8. mitigated and non-mitigated scenarios. In order to address these areas a limited number of situations requiring investigation were identified, including those which are described here i.e.: 1. high pressure releases, 2. small foreseeable releases, 3. catastrophic releases, and 4. the effects of walls and barriers. The numerical and experimental results of the project were ultimately used to derive recommendations which were an input to the IPG [1], in addition the work contributed to the overall advancement of knowledge in the area of H_2 safety. The key outputs of four of the scenarios are summarised in the following sections, references are given where work is further described elsewhere.

2. HIGH PRESSURE RELEASES

2.1 Overview and objectives

This work relates to the failure of high pressure H_2 storage. Pressures up to 900 bar (INERIS) have been investigated experimentally and pipe diameters up to 10 mm (Health and Safety Laboratory [HSL]). Data from the literature was used for model validation by both CEA and the University of Ulster [UU]). The aim of this scenario was to assess the hazard on failure of pipe-work/components and how the risk of this hazard can be minimised. Phenomena related to high pressure releases were studied, specifically jet fires, unignited jets, and the delayed ignition of the flammable cloud formed by a release. The work carried out focused on a better understanding and hence evaluation of the risks associated with high pressure releases. This in turn enables the estimation of safety or set-back distances for a range of situations.

2.2 Methodology

2.2.1 HSL Experiments

Release scenarios investigated included the effects of jet attachment and of varying; orifice size ignition delay, and ignition position. The flammability envelope, flame size, and heat fluxes for various geometries, and pressures were investigated. Restrictors of 1.5, 3.2, and 6.4 mm were used. Releases were also made at 9.5 mm (full bore). Tests using different ignition timings were performed with a single ignition position. Tests using a fixed ignition time were performed with varying ignition positions. The effects of jet attachment were evaluated by comparing jets released at 1.2 m height from the ground with jets released along the ground. All tests were performed with H_2 released at 205 bar into free air. Initial tests used an electrical ignition system; subsequent tests were performed with a pyrotechnic system. The following parameters were measured [3]: 1. Blast overpressure 2. Flame length (using a combination of low light and infra-red videos), 3. Infra red imaging, and 4. Background oriented Schlieren was performed on selected tests.

2.2.2 INERIS Experiments

The consequences of a high-pressure H_2 release that rapidly finds an ignition source were examined; flame length and radiation were investigated [3, 7]. Fig. 1 gives a schematic aerial view of the facility.

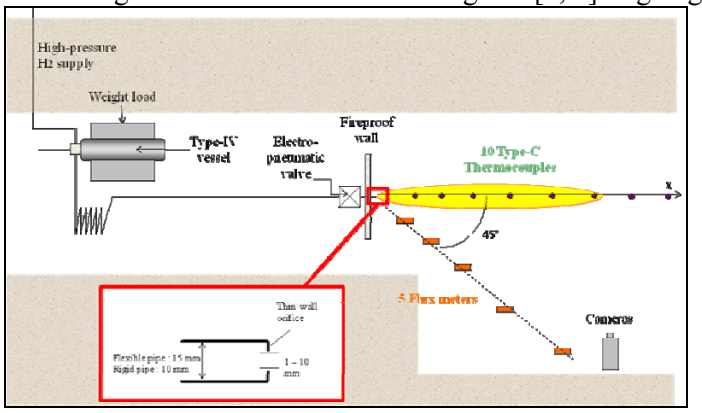

Figure 1: INERIS facility

Tests were carried out in an 80 m long gallery with a cross sectional area of approx. 12 m^2 in order to control the ambient conditions and to confine any effect that may arise from an unforeseen explosion. Low pressure (LP) tests (maximum pressure 100 bar) and high pressure (HP) tests (maximum pressure 900 bar) were performed. During the LP tests the bottle was connected to the nozzle orifice via a 15 mm diameter flexible pipe with an approx. length of 5 m.

Thin-wall orifices of 4, 7 and 10 mm were fitted at the release point. For the HP tests, the flexible pipe was replaced by a rigid one of similar length and internal diameter of 10 mm. Orifices of 1, 2 and 3 mm were used. The jet issued horizontally approx. 1.5 m above ground level and was ignited very

rapidly by a gas burner. To characterise the jet flame, 10 thermocouples and 5 fluxmeters were used. Visible and infrared cameras were positioned in a small recess within the gallery to visualise the flame

2.2.3 CEA simulations

The objective of CEA's simulation work was firstly to evaluate the consequences of a H_2 dispersion cloud in a large domain around a jet, and secondly to model the Takeno experiments of delayed ignition [8]. In the unignited case, an analytic model by Harstad [9] of the highly compressible part of the jet was used to provide input data for a CFD simulation. Turbulence was modelled using a k-ε approach. The commercial FLUENT code [10] was used. The scenario corresponds to the rupture of high pressure 10 mm piping, with an upstream pressure of 400 bar. It was supposed that a safety valve isolates the pipe within 2 s. The release direction was horizontal and a logarithmic variation of wind was considered. In Takeno [8] the delay before ignition is sufficient to assume that a premixed flame occurs. The model used here was a reactive fully compressible model, available in the CEA code Cast3m [11], implementing a CREBCOM [12] combustion model. The dispersion results were used as initial conditions for the combustion simulation. Ignition was assumed to take place 4 m from the nozzle on the axis of the jet, 2 s after the start of release. The average flame propagation velocity was approx. 325 m/s [8], this was used to correlate the parameter K_o of the CREBCOM model.

2.2.4 UU simulations

Simulations of free jet fires were carried out [2, 13]. Following a validation study, the approach was applied to predict flame length for a range of nozzle diameters, and stagnation pressures. The aim was to create a "nomogram" combining experimental and numerical results to approximate flame length for high momentum jet fires, and the extent to specific H_2 air concentration levels for unignited jets. Blowdown was not modelled in this case; pressure and temperature were taken to simulate a "quasi-steady" state, 3D LES were performed of the large scale turbulent non-premixed vertical H_2 jet fire. The CFD code FLUENT [10] was used. The modelling approach is described in [13], and includes an approach similar to Birch et al. [14] to calculate the equivalent diameter of the jet. Flame length was determined for a range of equivalent diameters from 0.1 mm up to 100 mm and the results of this study were combined with experimental data to generate a look up table.

2.3 Summary of results

2.3.1 HSL experiments

The results of the HSL experiments [3] are given in Tables 1-3. Unless otherwise stated the release height was 1.2 m, and the ignition point was 2 m from the release point. In Tables 2 and 3 a fixed orifice was used (6.4 mm). Table 3 shows the result of changing ignition position for a 6.4 mm orifice, and ignition delay of 800 ms. In all tests (Tables 1-3) the maximum pressures were recorded on sensor 1 (2.8 m from release point, 1.5 m from centre line of jet). The effect of attachment on jet length was also investigated. The attached jets were released along the ground at a height of 110 mm, and the unattached jets were released at a height of 1.2 m. Flame lengths of attached and unattached jets are given alongside additional experimental data in Figure 3. It can be seen that the flame lengths are longer in the case of attached jets by comparison to free jets.

2.3.2 INERIS experiments

Results for visible flame length have been plotted alongside additional experimental data in Figure 3. It should be noted that the data points plotted represent an average of every 5 recorded points. Though not represented here, two further observations were made: 1. a comparison of the visible and IR pictures showed that the most-radiating part of the flame has a shape similar to that of the visible flame. As pointed out in [15], this corresponds to the part of the flame where the temperatures are the highest since IR emissions result from vibrationally excited H_20* molecules that exist in high temperature combustion product,. 2. the maximum width of the flame was also found to be about 1/6 of its length. This is consistent with the observations given in [15].

Table 1: Maximum overpressure: vary orifice diameter and ignition delay

Orifice diameter (mm)	Ignition delay (ms)	Overpressure (bar)
1.5	800	Not recordable
1.5	400	Not recordable
3.2	800	0.035
3.2	400	0.021
6.4	800	0.152
6.4	400	0.027
6.4	400	0.037
9.5	800	0.165
9.5	400	0.049
9.5	400	0.054
9.5	400	0.033

Table 2: Maximum overpressure: vary ignition delay.

Ignition delay (ms)	overpressure (bar)
400	0.037
500*	0.184
600	0.194
800	0.152
1000	0.117
1200	0.125
2000*	0.095

* Denotes tests ignited by the electrical system

Table 3. Maximum overpressure: vary ignition position.

Ignition position (m)	Overpressure (bar)*
3	0.050
4	0.021
5	0.021
6	NR
8	NR
10	No ignition

*A pyrotechnic ignition system was used in these tests.

2.3.3 CEA simulations

Radial concentration in the dispersion calculations was compared to results of Chen and Rodi [16]. Reasonable agreement was shown up to 10 m from the jet exit, after which point buoyancy effects became significant and larger discrepancies appeared. Results were also compared to data of Takeno [8]. A direct comparison is difficult however, the extension of the flammable cloud was reasonably described (25 meters after 5 seconds), and the vertical motion of the cloud was overestimated. The maximum overpressures are presented in Figure 2 together with the experimental data of Takeno. It can be seen that the close-field behavior is well predicted on the coarse mesh, while the numerical data corresponding to both meshes deviate from experimental data for distances larger than 15m. Experimental data of Takeno show that the earlier the ignition time, the larger the maximum overpressure tends to be.

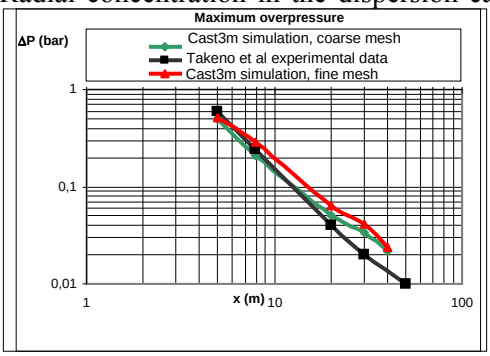

Figure 2: Comparison of numerical and Takeno maximum overpressure as a function of the distance from the ignition point

2.3.4 UU simulations and combined results on high pressure releases

The results of the UU simulations are shown alongside those of HSL, INERIS and data from the literature in Figure 3 which is an initial draft of an engineering nomogram. This is still under development by UU and further publications are under preparation to include existing engineering correlations. To use the nomogram the user should select only two parameters: the actual diameter of a release orifice (lower vertical axis), and tank pressure. Draw a horizontal line from actual leak diameter to a line corresponding to tank pressure, then continue the line vertically upwards until intersection with a line averaging experimental and simulated data, and from there draw a horizontal line to the left to estimate flame length. The same approach can be used to estimate the extent to 1% and 2% H_2 concentration.

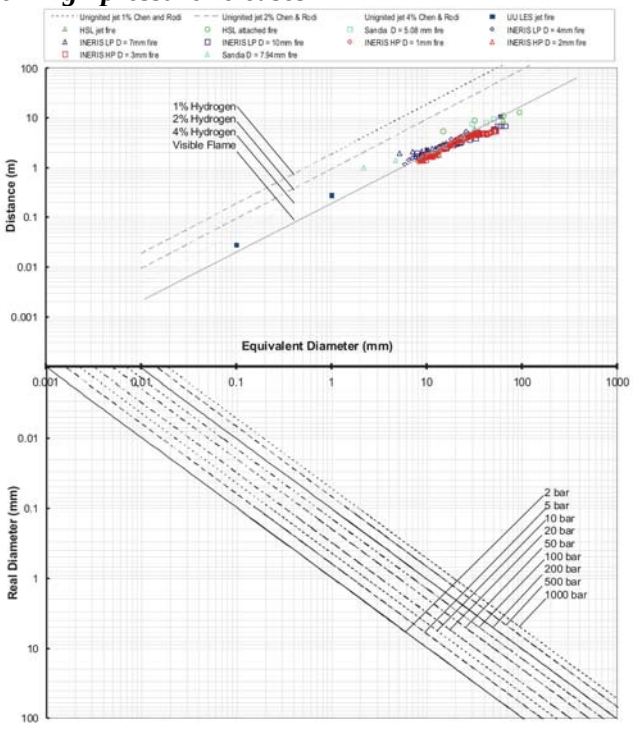

Figure 3: Engineering Nomogram

3. SMALL FORESEEABLE RELEASES

3.1 Overview and objectives

This scenario is concerned with "small" leaks that could potentially be controlled through ventilation. The areas of interest covered by this scenario relate to the low-pressure H_2 downstream of the pressure regulation controlling the flow of H_2 to the FC system (leaks originating inside the FC enclosure). The experimental and modelling work in this scenario included investigating dispersion of a H_2 leak and natural (NV) and forced ventilation (FV). Experiments were performed at the University of Pisa (UNIPI) and simulation work was performed at The National Centre for Scientific Research Demokritos (NCSRD) and UU. The work focused on the case of a FC system located inside a typical room or enclosure. The ventilation configurations in the room were varied to assess the resultant concentration of H_2 for different low leak rates.

3.2 Methodology

3.2.1 UNIPI experiments

Tests were conducted to determine the ventilation requirements in enclosures containing FCs, such that in the event of a foreseeable leak, the concentration of H_2 in air for zone 2 ATEX (2% v/v) [17] is not exceeded. A FC was placed inside the enclosure as shown in Figure 4. The leak rate, vent area (minimum of 0.35 m^2 and maximum of 2.5 m^2), and vent location were varied. The most credible loss of H_2 is at the valve of the inlet gas pipeline. A worst case value of 5 bar was taken to calculate the leak. The leak area was calculated as 0.25 mm^2 using ATEX guidance for small accidental leaks from valves, resulting in a flow rate of no more than 40 l/min (calculated with EFFECTS-GIS 7.3). Larger leaks through areas of 0.5 and 1.0 mm^2 were also tested. H_2 concentration was measured at 5 locations as shown in Fig. 4. In the case of NV three flow rates were considered: small (GH2s) = 40 nl/min, average (GH2a) = 90 nl/min, and big (GH2b) = 180 nl/min.

For FV the main parameters are the same as NV, additionally two fan flow rates were considered: small air flow = 0.3 m^3/s (AFs); big air flow 0.6 m^3/s (AFb). For NV the initial value of the vent size was compared with the indication of the norm ATEX and Q_{aw} is defined as the NV air flow rate. This norm suggests empirical formulas applicable to various geometries, details on the calculations can be found in [17]. Where the natural recirculation fails the FV experiments have been performed to complete the experimental matrix to measure H_2 %vol < 2% as the ATEX zone 2 prescribes. Note vent area is indicated in Fig. 4.

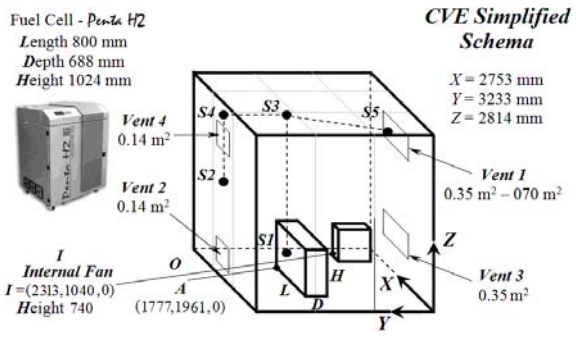

Figure 4: Location of the sampling points and size of the four vent areas (not to scale)

3.2.2 NCSRD simulations

The majority of UNIPI's NV experiments were simulated by NCSRD [2, 18] using the ADREA-HF code [19]. Validation studies of the code for gaseous H_2 release and dispersion can be found in [20, 21]. The modelled facility is shown in Fig. 5, and includes the full interior of the FC, in order that potential accumulation effects may be investigated. A volume porosity and area permeability approach was used to model the complex geometrical layout with a cartesian grid. Turbulence was modelled using the standard k-ε model [22] modified for buoyancy effects.

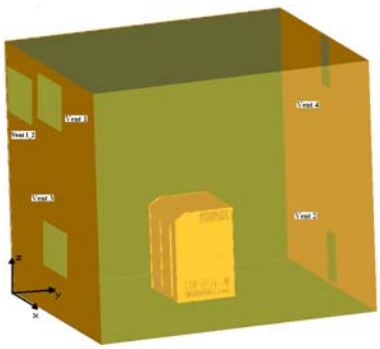

Figure 5: Facility and FC (DELTA-B Code)

3.2.3 UU Simulations

In real situations wind may hamper or worsen the effectiveness of NV, leading to higher H_2 concentrations in the facility where the leak occurred. Simulations were performed by UU to investigate the effect of wind on the efficiency of NV. Wind was directed along the 0Y axis (oncoming at a right angle to the upper vent). The vertical wind velocity profile was defined as, $u(z) = (u_* / k)\ln(z/z_0)$ where $u(z)$ is the horizontal wind speed at height z, k=0.40 is the von Karman constant, and z_0 =0.03 m is the characteristic roughness of the ground [23], 4 steady state simulations were conducted air velocities of approximately 0, 0.11, 0.33 and 1.1 m/s respectively at z=2.5 m.

3.3 Results

3.3.1 UNIPI experiments

In Table 4 the geometrical configuration is correlated with the theoretical ventilation ATEX value Q_{aw} and the efficiency of NV is given for three H_2 leakage rates. The volume of the reference enclosure is 25 m^3 with vent areas as illustrated in the column "Configuration". The NV is deemed to be "Effective" only if ATEX zone 2 is respected. The reader is referred to Fig. 4 for vent areas. In conclusion the NV, as described in ATEX norm [17] zone 2 is effective when considering the worst leak (40 l/min) from the 5 bar pipe, except in case 1. For a leak of 90 l/min the NV is effective only in case 10 and the NV is always ineffective considering a leak of 180 l/min. The results of FV tests are shown in Table 6. For each test the direction and type of FV is shown.

Table 4. Results of natural ventilation tests.

Configuration 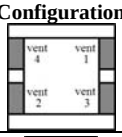	**ATEX calculation of air-flow recirculation Q_{aw} referred to wind speed (W) = 1 m/s**	**Theoretical ATEX value of Q_{aw} (m^3/s)**	**NV 40 l/min** Efficient Y/N	**NV 90 l/min** Efficient Y/N	**NV 180 l/min** Efficient Y/N
	$Q_{aw} = 0.025\ A\ W$ $A = V1$	0.009	N	N	N
		0.018	Y	N	N
	$Q_{aw} = c_s\ A_{aw}\ W\ (\Delta c_p)^{0.5}$ $\frac{1}{A_{aw}^2} = \frac{1}{V1^2} + \frac{1}{V2^2}$, $\Delta c_p = 0.2$, $c_s = 0.65$	0.037	Y	N	N
		0.04	Y	N	N
	$Q_{aw} = 0.025\ A\ W$ $A = V1 + V3$	0.018	Y	N	N
		0.026	Y	N	N
	$Q_{aw} = c_s\ A_{aw}\ W\ (\Delta c_p)^{0.5}$ $\frac{1}{A_{aw}^2} = \frac{1}{V1^2} + \frac{1}{V4^2}$, $\Delta c_p = 0.2$, $c_s = 0.65$	0.037	Y	N	N
		0.04	Y	N	N
	$Q_{aw} = c_s\ A_{aw}\ W\ (\Delta c_p)^{0.5,}$, $\Delta c_p = 0.2$, $c_s = 0.65$ $\frac{1}{A_{aw}^2} = \frac{1}{(V1+V3)^2} + \frac{1}{(V2+V4)^2}$	0.07	Y	Y	N
		0.08	Y	Y	N

Table 6. Results of forced ventilation tests.

Configuration	**Direction of air-flow Fan area A_f = 0.05 m^2**	**Free vent area Av (m^2)**	**Fan air-flow, Internal value of Q_{aw} (m^3/s)**	**NV 40 l/min** Efficient	**NV 90 l/min** Efficient	**NV 180 l/min** Efficient
		0.14	0.66	Y	Y	N
		0.14	0.33	Y	Y	N
		0.35	0.33	Y	Y	N
		0.49	0.66	Y	Y	N
		0.28	0.66	Y	Y	Y
		0.89	0.33	Y	Y	Y

3.3.2 NCSRD simulations

In general reasonably good agreement was found between predicted and experimentally measured concentration time histories for all simulated cases. Results from two of the simulations are presented below for test 3 and test 11. For test 3 the release flow rate was 40 l/min, the nozzle diameter 1 mm and vent 1 was open. For test 11 the release flow rate was 90 l/min, the nozzle diameter 6 mm and both vents 1 and 2 were open. In both tests, the release was inside the FC with a horizontal direction. Figures 6 and 7 depict the H_2 volumetric concentration at sensors 2, 3, 4, and 5 of the UNIPI experiments and the NCSRD simulation results for Tests 3 and 11 respectively. For test 3 neither the experiments nor the simulations showed a H_2 concentration reaching 2%. For test 11, both the experimental and simulated value of sensor 3 did not exceed 2.5%. The experiment showed a slight excess of 2% of H_2 concentration for sensor 3 while sensor 5 almost reached that value. Both simulation and experiment show a decline in the H_2 concentration in all sensors after approximately 360 s. At this time there is a rapid decline of the release flow rate giving a zero flow-rate at 420 s.

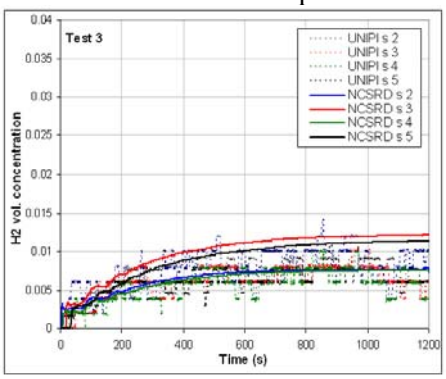

Figure 6: UNIPI-NCSRD comparison (sensors 2, 3, 4 and 5)

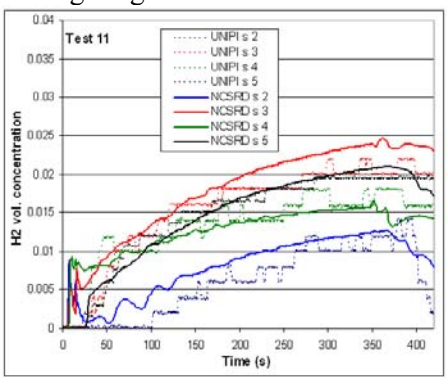

Figure 7: UNIPI-NCSRD comparison (sensors 2, 3, 4 and 5)

3.3.4 UU simulations

Fig. 8 illustrates the dependence of H_2 concentrations in the locations of Sensors 2 – 5 as a function of wind velocity. In the studied case the ambient wind worsens H_2 venting in a very narrow range of velocities: at a wind velocity of 0.33 m/s H_2 concentrations at Sensors 2-5 are restored to their values at quiescent conditions, due to more intensive venting through the lower vent and more intensive H_2 mixing. At a wind velocity u=1.1 m/s H_2 concentration decreases drastically due to intensive mixing within the CVE facility. The results show that although the ambient wind may decrease the rate of natural ventilation during a H_2 release, this effect is only observed in a narrow range of wind velocities.

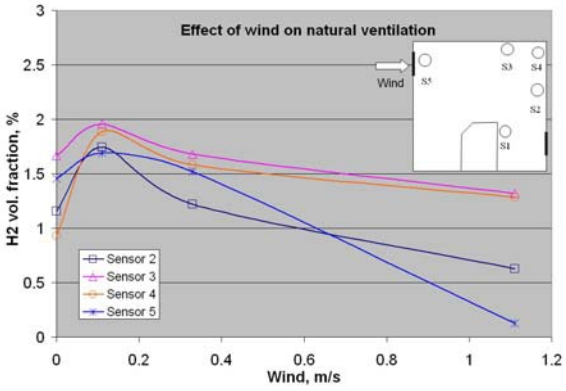

Figure 8: H_2 concentrations at sensors 2 – 5 as a function of inflow wind velocity

In a realistic scenario one might expect this effect to be diminished even further as a result of turbulent fluctuations in atmospheric wind both in velocity direction and value

4. CATASTROPHIC RELEASES

4.1 Overview and objectives

Rupture of a H_2 feed line inside the FC enclosure was considered. Experiments were performed by Pro-Science [24] whereby H_2 release rates of up to 15 g/s were considered for a duration of 1 s. Both dispersion and subsequent ignition of the H_2 air mixture was considered for different configurations and flow rates. Modelling work by CEA included validation and assessment of overpressures.

4.2 Methodology

4.2.1 Pro-Science experiments

The hazard potential of a severe H_2 leakage inside a FC cabinet was investigated using a generic FC enclosure model with an internal volume of approx. 560 l. In all cases 120 l of this volume were blocked by a solid cube representing large internals of the FC. Based on the description of a

commercially available FC unit the max. H_2 release rate in case of a rupture of the feed line inside the enclosure was evaluated to 15 g H_2/s. Therefore H_2 release rates from 1.5 to 15 g H_2/s were used. A security mechanism was assumed to shut down the H_2 supply after 1 s. Three cases with different venting characteristics were investigated: In case 1 two vent openings were arranged diagonally on opposite sides of the enclosure; passive (case 1a) and active venting (case 1b, with 2 fans mounted at the vent openings) was investigated. In case 2 enlarged vent openings with doubled size at the same positions were used (passive venting), and in case 3 an additional chimney was fixed on the top of the enclosure with the smaller vent openings in the sidewalls (passive venting).

Dispersion experiments were performed and H_2 concentration was determined at certain positions in- and outside the enclosure, 2 internal geometries were investigated. In the low obstructed internal geometry a grid cube consisting of intersecting obstacles (BR 50%) was mounted at the top of the model enclosure, reducing the gas volume inside the enclosure to approx. 380 l. In the highly obstructed internal geometry the entire free space inside the enclosure was occupied by grids (BR 50%), reducing the gas volume inside the enclosure to approx. 240 l. In the combustion experiments 2 scenarios differed by the location of the ignition point were investigated. In scenario C the ignition position was located inside the enclosure, close to the upper left front edge. In scenario D outside ignition positions, situated above the centre of the upper vent opening or above the centre of the chimney were used. With these ignition positions two ignition times were studied: In experiments with a delayed ignition the ignition source was turned on 4 s after the beginning of an experiment for 300 ms. In the distribution experiments the highest H_2-concentrations most often were observed between 2 and 6 s after an experiment was started. In experiments with a durable ignition the ignition source was turned on simultaneously with the beginning of the H_2 release for duration of 5 s to take into account possible ignition sources that are permanently present (e.g. hot surfaces).

4.2.2 CEA simulations

Both distribution and combustion phases of two Pro-Science experiments on case 1a with a H_2 release rate of 6 g/s and an ignition after 4 s were modeled. The experiments were performed with the ignition source located either inside the enclosure or above the upper vent opening. The commercial code FLUENT was used for the dispersion phase [10]. As described in Section 2.3.3 the CEA code Cast3m was used for the combustion phase implementing a CREBCOM combustion model. A 3D model was created to represent the Pro-Science experiments. The upper and lower vents were modeled and the stack was represented by a solid block, while the upper grid was represented as a porous medium. The leak was horizontal, 8 mm diameter, located 0.475 m from the bottom of the model, and oriented toward the inside of the FC. The H_2 flow rate was 6 g/s for 1 s. The Birch model [14] was used to determine an equivalent velocity and source area. A k-ε model was used for turbulence.

4.3 Results

4.3.1 Pro-Science experiments

Due to the buoyancy of the released H_2 and FV a so called “chimney effect” was observed in all experiments with the low obstructed internal geometry [24]. In case 3 the additional chimney took the role of the upper vent opening. In the experiments with the highly obstructed internal geometry, where the vent openings were partially blocked by the grid, the mentioned chimney effect was not observed, and, compared to the experiments with low obstruction, outside the enclosure only small H_2 concentrations were measured. At the same time inside it an inhomogeneous mixture distribution with very high H_2 concentrations close to the walls and beneath the top were observed. Compacting the obstacles would minimise the hazard of possible flame acceleration in distributed obstructed areas and would also allow to avoid an obstruction of the vent openings. Due to the high H_2 concentrations found inside the enclosure in the distribution experiments with the highly obstructed internal geometry it was decided not to perform combustion experiments with such internal geometry. The 3 main venting characteristics investigated showed little difference concerning the max. H_2 concentrations measured; however differences in the H_2 transport to the outside of the enclosure and in the homogeneity of the H_2 distribution were recognised [24]. In the combustion experiments cases 1a and 2 generated similar loads, but different combustion behaviours were found in some of the experiments on cases 1b and 3. [24] The active venting used in case 1b is responsible for a comparably slow combustion with a released H_2 amount of 1.5 g and durable internal ignition. With the higher H_2

amount of 3 g the flame velocities determined inside the enclosure model were similar to the ones of the corresponding experiments in the cases 1a and 2. The opposite effect of the active venting was found in experiments with durable outside ignitions. For delayed ignitions similar combustion behaviours as in the other cases were observed. The slowest combustions were observed for delayed outside ignitions, while the highest loads were detected with a durable internal ignition. With the latter ignition settings combustion was detected by all the sensors even in experiments with a H_2 amount of 1.5 g. The ignition of 3 g H_2 resulted in pressure waves with a max. amplitude of 40 mbar inside the model enclosure; such pressure loads can cause glass breakage of large windows [25]. For a H_2 release of 4 g and durable internal ignition pressure waves with a max. amplitude of approx. 100 mbar were observed inside the enclosure, which may even lead to injuries to human beings [26].

4.3.2 CEA simulations

Fig. 9 shows the simulated 4% isosurface after 0.31 s and 21.5 s. The flammable cloud exits the FC by the lower vent from 0.25 s to 3.2 s, then the flow is reversed and fresh air enters the cell. The flammable cloud exits the FC by the upper vent at 0.5 s and after 20 s the flammable cloud still occupies the upper part of the FC. So qualitatively, the experimental results were recovered.

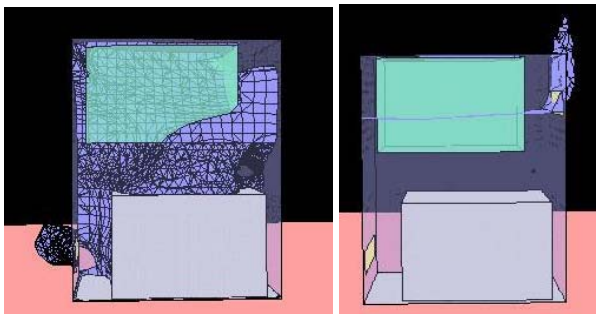

Figure 9: Isosurface 4% H_2 after 0.31 s (L), and 21.5 s (R)

To compare the concentrations measured, calculated concentrations were averaged over the corresponding time period of the measurements. The experimental and simulated results showed good agreement. In the simulation, the flammable mass reaches a max. of nearly 6 g after 1 s and then decreases slowly. After 4 s, when ignition occurs, the flammable mass of H_2 is predicted to be 5.5 g. This prediction could not be verified experimentally. Concerning the combustion modelling, the main difficulty was to estimate the amount of H_2 which is inside the cell at ignition time because a certain quantity escapes through the openings. The strategy employed was i) to choose several values of H_2 molar fraction (under hypothesis of homogeneously distributed H_2 inside the cell), ii) to determine the flame velocity using correlations available from the literature [27], and iii) to compute the pressure evolutions at certain positions inside/outside of the FC using two geometries: one which takes into account only the FC, and the other the outside domain as well. This strategy provides conservative pressure estimations. The calculation results show that flame acceleration occurs in the cube obstacle and close to the rear wall leading to high overpressures. For a remaining H_2 mass of 4 g within the FC, the predicted overpressure is 0.2 bar, this is consistent with the measurements. For higher H_2 inventories, i.e. 7 g and 9 g, the overpressure is predicted to be up to 15 bars due to shock focusing in the corner of the FC where the transducer is installed if the structure is supposed rigid.

5. THE EFFECT OF WALLS AND BARRIERS

5.1 Overview and objectives

H_2 jet flames resulting from the ignition of unintended releases can be extensive in length and pose significant radiation and impingement hazards [15, 28]. Depending on the leak diameter and source pressure the resulting consequence distances can be unacceptably large [29]. One mitigation strategy is to incorporate barriers around H_2 storage equipment, as walls may reduce the extent of unacceptable consequences due to jet releases resulting from accidents involving high-pressure equipment. The objectives of this scenario were to: determine barrier wall effectiveness, determine the resulting overpressures and radiation, and consider the effect of various angles of impingement. The experimental work was carried out predominantly by Sandia [31, 32] and complementary activities were undertaken at HSL. Simulation work was carried out at Sandia and a case was modelled by FZK.

5.2 Methodology

5.2.1 Sandia experimental and modeling programme: Overview of activities and some results

A combined experimental and modelling programme was undertaken to better characterise the effectiveness of barrier walls to reduce hazards. The experimental measurements include flame

deflection using standard and infrared video and high-speed movies (500 fps) to study initial flame propagation from the ignition source. Measurements of the ignition overpressure, wall deflection, radiative heat flux, and wall and gas temperature were also made at strategic locations. The modelling effort included 3D calculations of jet flame deflection by the barriers, computations of the thermal radiation field around barriers, predicted overpressure from ignition, and the computation of the concentration field from deflected unignited H_2 releases. Four barrier tests were carried out with various wall heights and orientations using high-speed video and other suitable transducers to characterise the flame and wall interactions. The configurations of the barrier wall tests are shown in Fig. 10. A fifth test was also performed for a free H_2 jet flame with no wall present to provide baseline data for evaluating the effectiveness of the barrier walls at hazard mitigation. The data obtained during the tests provides a basis for direct evaluation of barrier effectiveness for flame hazards mitigation associated with accidental H_2 leaks, as well as providing data for model validation. Simulations of the barrier experiments were performed with the Sandia developed code, FUEGO, designed to simulate turbulent, reacting flow and heat transfer [32]. These simulations were made prior to performing the tests and were used to help guide the proper placement of sensors for the experiments. Comparisons of the video clips from the tests with temperature colour contour plots indicate that the model correctly predicts the deflected jet flames observed in the experiments. The amount of overpressure produced from the ignition of the impinging jet release into the barrier was also studied using the FLACS Navier-Stokes code [33]. Simulated peak overpressures on the front side of the barrier were found to be approximately 39 kPa for the 1-wall vertical barrier (Test 1) as compared to approximately 41 kPa for the 3-wall barrier (Test 5) configuration. This is illustrated in Fig. 11.

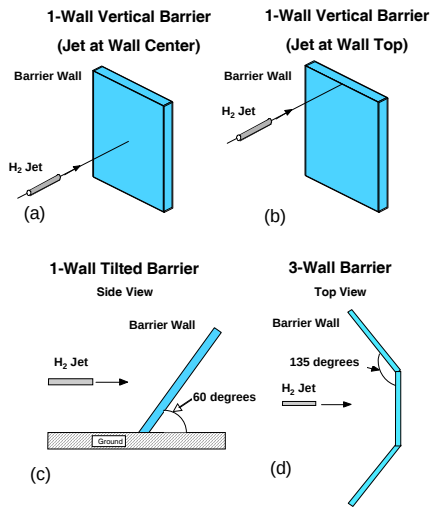

Figure 10: Schematics of barrier wall configurations for tests and calculation

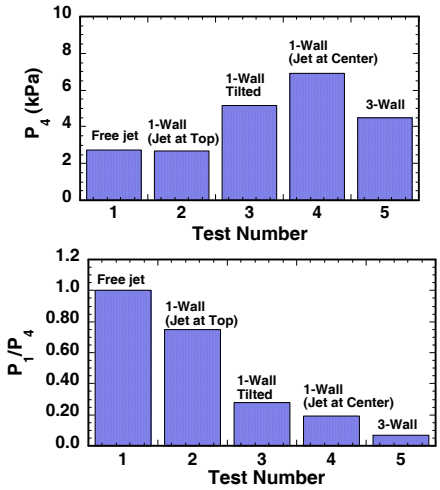

Figure 11: Overpressures measured in a free jet and each of 4 barrier wall configurations. Top graph: Max. overpressure measured prior to wall; Lower graph: Ratio of max. overpressure measured after the wall to that prior to the wall.

5.2.2 FZK simulations: Overview

Two geometry configurations were chosen to be modelled by FZK [2], i.e. the free jet configuration (a) in Fig 10. The calculations were divided in two sections: in the first phase the ability of the code to model the jet dynamics was checked ("cold") and in the second phase which combustion was studied ("hot"). The COM3D code was used. To provide data on dynamics of explosion, taking into account different levels of accumulation of fuel, three moments of ignition were selected for the geometrical configurations i.e. 140 ms, 260 ms and 640 ms. In both cases the grid was cubic with a cell size of 4 cm. Due to the lack of resolution; a coarse model was used for the real nozzle. The mass flow rate was preserved equal to the value estimated from the experiments. The model nozzle was located at a distance 20 cm downstream the original nozzle location. The convective part of the Navier-Stokes equations, was calculated with the explicit second order TVD numerical scheme. Simulations were performed using a standard k-ε model. A virtual one cell ignition source was established in the

calculations, in which a prescribed reaction rate is introduced. For simulation of combustion the semi-empirical KYLCOM model was selected. Where flame speed is modelled as a function of turbulence. In general it was found that: The proposed models and tools produce satisfactory results even in coarse meshes, the dispersion and combustion process has acceptable accuracy for practical purposes of safety analysis.

6. CONCLUSIONS

Considering high pressure releases: The engineering nomogram given in Figure 3, combines the data of CEA, UU and HSL with that from the literature and can be used to estimate flame length, or extent of the flammable envelope to 1%, 2% and 4% H_2 for a given storage pressure and diameter. In addition a number of specific recommendations have been drawn from HSL's experimental programme: 1. the inclusion of flow restrictors in H_2 supply lines reduces the flame lengths observed. 2. When a release is orientated such that attachment to a surface can occur the jet length may be enhanced. 3. Ignition in a weak region of the jet cloud results in a relatively slow burn and hence a small overpressure. 4. Max. overpressures were observed when the jet was ignited at a time coinciding with the area of maximum turbulence within the front portion of the jet, reaching the ignition point.

For small foreseeable releases: The analysis of the natural and forced ventilation efficiency suggests adopting this safety system in all enclosures where a credible non-catastrophic leakage can occur. Where it is possible, it is convenient to use one or more suitable solutions for example: 1. reasonably increase the vent areas beyond the min. value calculated using ATEX; 2. consider the vent areas for a leak flow reasonably bigger then the min.; 3. incline the roof making the NV easy and efficient, 4. install a small fan able to remove the internal mixture from the enclosure. The limit of 40 l/min of the leakage is referred to an every kind of FC suitable for civil use, it is reasonable to consider leaks no bigger then 90 l/min as such a value refers to a catastrophic leakage**.**

The experiments on catastrophic releases have demonstrated that to diminish possible hazards it is necessary to reduce the H_2 amount that can be released from a ruptured pipe inside the FC enclosure to below 1.5 g. This investigation leads to several recommendations: 1. the feed line pressure and/or diameter should by design limit the flow rate to what is necessary for FC consumption. In the case studied here, a target inventory of 1 g is recommended. 2. The release duration should be reduced as much as possible. 3. obstacles should be avoided by a careful design of the cell itself. 4. vent design should allow for a rapid dispersion of H_2 during a leak and efficient pressure relief during an explosion.

Considering the effect of walls and barriers: For the conditions investigated, 13.79 MPa source pressure and 3.17 5mm diameter round leak, the barrier configurations studied were found to 1.reduce horizontal jet flame impingement hazard by deflecting the jet flame, 2. reduce radiation hazard distances for horizontal jet flames, 3. reduce horizontal unignited jet flammability hazard distances. For the 1-wall vertical barrier and 3-wall barrier configurations the simulations of the peak overpressure hazard from ignition were found to be approx. 40 kPa on the release side of the barrier and approx. 5-3 kPa on downstream side of the barrier.

Overall the activities performed within HYPER provided both experimental and numerical insight into the key scenarios related to the safety of stationary FC installations. While practical guidelines concerning the design and installation of FCs were provided, given the short duration of the project all knowledge gaps could not be solved. Therefore there is a need for further experimental and numerical investigations, particularly to gain better understanding of the basic underlying physical phenomena, and further examine mitigation effects including ventilation and barriers.

7. ACKNOWLEDGEMENTS

The support of the European Commission through the FP6 STREP HYPER project is greatly appreciated (http://www.hyperproject.eu/, http://epshypp.web.its.manchester.ac.uk/)

8. REFERENCES

1. HYPER Installation Permitting Guidance for Hydrogen and Fuel Cells Stationary Applications, January 2009, available at http://www.hyperproject.eu/
2. HYPER D4.3 Releases, Fires, and Explosions, Final Modelling Report, August 2008

3. HYPER D5.2 Report on High Pressure and Catastrophic Releases, September 2008
4. HYPER D5.3 Report on small scale releases, September 2008
5. HYPER D5.4 Report on Safety Barrier Hydrogen Release Interaction, September 2008
6. HYPER D1.2 Gap Analysis / Priorities Report, February 2007
7. Proust C. and Studer E. High pressure hydrogen fires, 3rd ICHS, 2009 Corsica, France
8. Takeno K. et al. Phenomena of dispersion and explosion of high pressurized hydrogen, 2nd ICHS, 2007 San Sebastian, Spain.
9. K. Harstad, J. Bellan, Global analysis and parametric dependencies for potential unintended hydrogen fuel releases, Combustion and Flame, 144, pp.89-102, 2006.
10. Fluent Inc. Fluent 6.3 User Manual
11. Cast3m web site http://www-cast3m.cea.fr/
12. Efimenko A. A., Dorofeev S. B, CREBCOM code system for description of gaseous combustion. Journal of Loss of Prevention in the Process Industries. Vol.14, 2001
13. Brennan S., Makarov D, and Molkov V. LES of high-pressure hydrogen vertical jet fire, Journal of Loss Prevention in the Process Industries, Volume 22, Issue 3, May 2009, Pages 353-359
14. Birch A. D., Hughes D. J., Swaffield F., Velocity Decay of High Pressure Jets, Combustion Science and Technology, 52, 1987, pp 161-171
15. Schefer, R.W., Houf, W.G., Bourne, B., and Colton, J., Spatial and Radiative Properties of an Open-Flame Hydrogen Plume, Intl. Journal of Hydrogen Energy, Vol. 31, 1332-1340, 2006.
16. Chen C. J. and Rodi W. Vertical Turbulent Buoyant Jets - a Review of Experimental Data, 1980, Oxford, Pergamon Press.
17. ATEX guide of reference CEI EN 60079-17; CEI 31-35:2001-01 (ITA).
18. Papanikolaou E., Venetsanos, A. G., Cerchiara G. M., Carcassi M and Markatos N, CFD Simulations on Small Hydrogen Releases inside a Ventilated Facility, 3rd ICHS , France, 2009
19. Papanikolaou, E., Venetsanos, A., Carcassi M., Cerchiara G., Markatos, N., Venetsanos, A., Huld, T., Adams, P., Bartzis, J.G., Source, dispersion and combustion modelling of an accidental release of hydrogen in an urban environment:, Journal of Hazardous Materials, Vol. A105, 2003, pp. 1-25
20. Gallego, E., Migoya, E., Martin-Valdepenas, J.M., Crespo, A., Garcia, J., Venetsanos, A., Papanikolaou, E., Kumar, S., Studer, E., Hansen, O.R., Dagba, Y., Jordan, T., Jahn, W., Hoiset, S., Makarov, D., Piechna, J., An intercomparison exercise on the capabilities of CFD models to predict distribution and mixing of H_2 in a closed vessel, 1st ICHS, Pisa, Italy, 2005
21. Papanikolaou E.A. and Venetsanos A.G., CFD modelling for helium releases in a private garage without forced ventilation, 1st ICHS, Pisa, Italy, 2005
22. Launder B.E. and Spalding D.B., The numerical computation of turbulent flows, Computer Methods in Applied Mechanics and Engineering, Vol. 3, Issue 2, 1974, pp. 269-289
23. Hanna S.R., Britter R.E., Wind Flow and Vapour Cloud Dispersion at Industrial and Urban Sites, CCPS, ISBN 0-8169-0863-X.
24. Friedrich A., Veser A., Kotchourko N., and Stern G., HYPER experiments on catastrophic hydrogen releases inside a fuel cell enclosure, 3rd ICHS, Corsica, France, 2009
25. Baker, W. E., Cox, P.A., Westine, P.S., Kulesz, J.J. and Strehlow, R:A., Explosion Hazards and Evaluation, 1983, Elsevier Scientific Publishing Co., Amsterdam, The Netherlands.
26. Richmond et al., Physical Correlates of Eardrum Rupture, Blast Injuries of the Ear Seminar, Walter Reed Army Medical Center, Washington, DC, Sept 26-27, 1986
27. Dorfeev S.B., Evaluation of safety distances related to unconfined hydrogen explosions. Intl. Journal of Hydrogen Energy 32 2118 – 2124, 2007
28. Schefer, R., Houf, W.., Williams, T., Bourne, B., and Colton, J., Characterization of High-Pressure, Under-Expanded Hydrogen-Jet Flames, Intl. Journal of Hydrogen Energy, Vol. 32, 2081–2093, 2007
29. Houf, W., and Schefer, R., Predicting Radiative Heat Fluxes and Flammability Envelopes from Unintended Releases of Hydrogen, Int. Jour. of Hydrogen Energy, Vol. 32, 136-151, Jan 2007.
30. Houf, W. G, Evans G. H., Schefer R. W., Merilo E., and Groethe M., A Study of Barrier Walls for Mitigation of Unintended Releases of Hydrogen, 3rd ICHS, Corsica, France, 2009
31. Schefer R. W., Merilo E., Groethe M., and Houf W. G., Experimental Investigation of Hydrogen Jet Fire Mitigation by Barrier Walls, 3rd ICHS, Corsica, France, 2009
32. Moen, C, Evans, G., Domino, S. and Burns, S.., A Multi-Mechanics Approach to Computational Heat Transfer, proceedings 2002 ASME Int. Mech. Eng. Congress and Exhibition, IMECE2002-33098
33. FLACS Version 8 Users Guide, Gexcon, Bergen, Norway, 2003.